SciDAC: Topological and Correlated Matter via Tensor Networks and Quantum Monte Carlo

Joel Moore
UCB/LBL

Chunjing Jia
SLAC

Hongchen Jiang
SLAC

Steve Kivelson
Stanford/SLAC

Dung-hai Lee
UCB/LBL

Brian Moritz
SLAC

Donna Sheng
CSUN

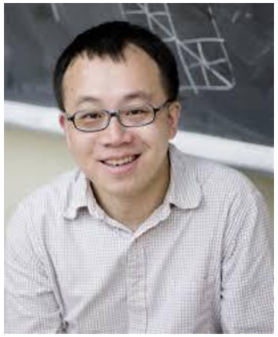

Lexing Ying
Stanford

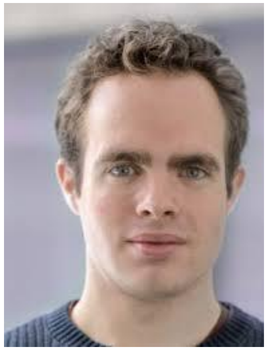

Mike Zaletel
UCB

Hubbard model

SciDAC: Topological and Correlated Matter via Tensor Networks and Quantum Monte Carlo

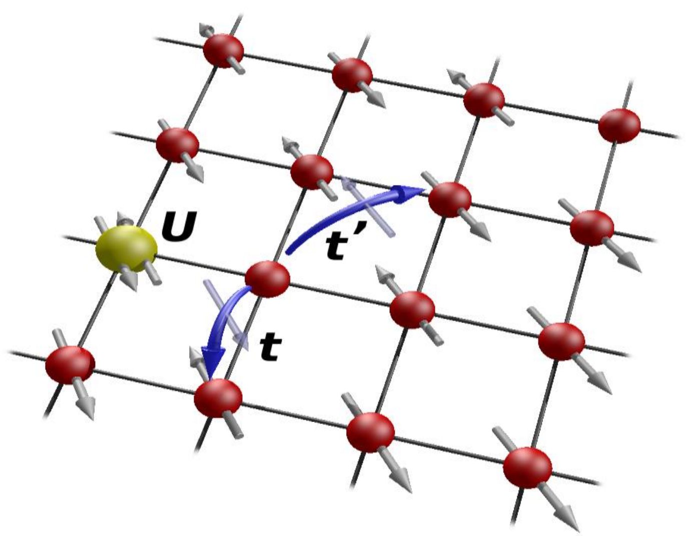

Simplest model of interacting particles on a lattice.

Surprisingly few exact solutions.

Rich possibility of phases - Eg: magnetism, charge order, superconductivity, spin liquids, ground state degeneracies, topological order

Premium on methods that capture the full Hilbert space of a quantum system that scale more efficiently than diagonalization.

Goals:

- **develop Tensor Network methods that generalize Density Matrix Renormalization Group (DMRG) methods**
- **Perform fermion-sign free quantum Monte Carlo and benchmark DMRG**

Algorithmic advances – 2D Tensor Networks

A central goal of SCIDAC: generalizing the success of DMRG to 2D materials using "2D tensor networks"

Decade old idea, but stable & efficient numerical scheme was elusive

Zaletel has developed a variant of the 2D tensor network ansatz which allows for efficient numerical manipulation:

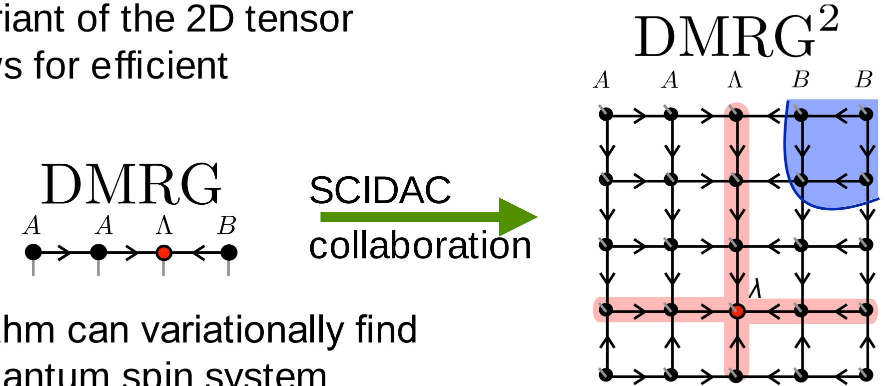

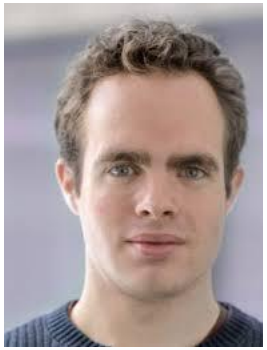

We demonstrate this algorithm can variationally find the ground state of a 2D quantum spin system without an exponential blow-up with system size

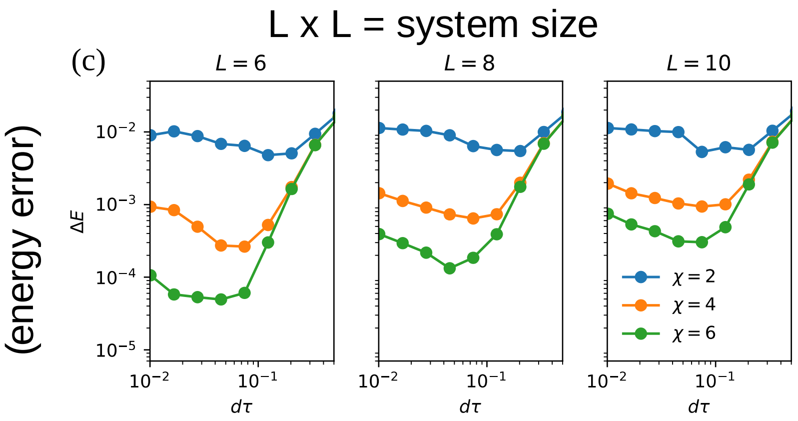

Energy errors on the order of 10^{-4}/ site obtained within an hour on single workstation

Focusing on scaling up implementation, "infinite size" algorithm, & generalizing to Hubbard model

From "Isometric tensor network states in two dimensions"

M. Zaletel and F Pollmann, **arXiv:1902.05100**

Algorithmic advances -iPEPS

We develop different variants of infinite projected entangled-pair state (iPEPS) ansatz to improve the efficiency of the tensor network.
In particular,

(i) we implement strategy to optimize tensors with U(1) symmetry and also introduce an optimization method to treat second-neighbor interactions more efficiently in full update of tensor.

(ii) For tensor contraction (overlap) calculations, we implement the single-layer tensor network based on the corner-transfer matrix technique.

(iii) Our benchmark results based on the full-update algorithm in comparison with DMRG show that the iPEPS can faithfully represent different quantum states of infinite systems, including magnetic ordered phases, stripe or valence bond solids as well as chiral spin liquids.

Reference
R. Haghshenas et al., Phys. Rev. B 97, 184436 (2018); R. Haghshenas et al., arXiv:1812.11436.

Algorithmic advances – DMRG

Various low-level optimizations have been performed

- Using a combination of OpenMP and batch-gemm, take advantage of block sparsity to gain speed.

- Employ more symmetries to gain two orders of magnitude in speed.
  For example, we have implemented SU(2) spin rotational symmetry in our new DMRG algorithm, including pure spin model, t-J and Hubbard models. This allows us to keep 2.7-4 times more number of states with significantly higher accuracy, and with around 20-100 times faster in speed

Both of these achievements help us to check for better and improved ground state convergence.

Next: parallelize to multinodes using high level optimizations.

Aaron Szasz, Johannes Motruk, Michael P. Zaletel, Joel E. Moore, **arXiv:1808.00463**

Hong-Chen Jiang, Zi-Xiang Li, Alexander Seidel, Dung-Hai Lee, Science Bulletin **63**, 753 (2018).

DMRG single-band Hubbard

Hong-Chen Jiang, TPD, arXiv:1806.01465, to appear in *Science*

Yi-Fan Jiang, Jan Zaanen, TPD, Hong-Chen Jiang, unpublished

$$H = -t\sum_{\langle ij\rangle} c^\dagger_{i\sigma}c_{j\sigma} + U\sum_i n_{i\uparrow}n_{i\downarrow} - t'\sum_{NNN} c^\dagger_{i\sigma}c_{j\sigma}$$

4 x L_x Hubbard ladders
(L_x = 16…96)
m = 4K…20K states
Truncation error ~ 10^{-7}
U/t = 8 … 12
t'/t = -0.25 … 0.05
Filling 1/12, 1/10, 1/8 holes

- Quantum phase diagram on 4-leg ladder
- Filled stripe phase (t’ close 0)
- Luther Emery Liquid phase (t’ = - 0.25t)
- Roles of t’ and U

doped t-J model - four-leg cylinders:

Hong-Chen Jiang, Zheng-Yu Weng, Steven A. Kivelson, PRB 98, 140505 (2018)

John F. Dodaro, Hong-Chen Jiang, Steven A. Kivelson, PRB 95, 155116 (2017)

CDW – role of t'

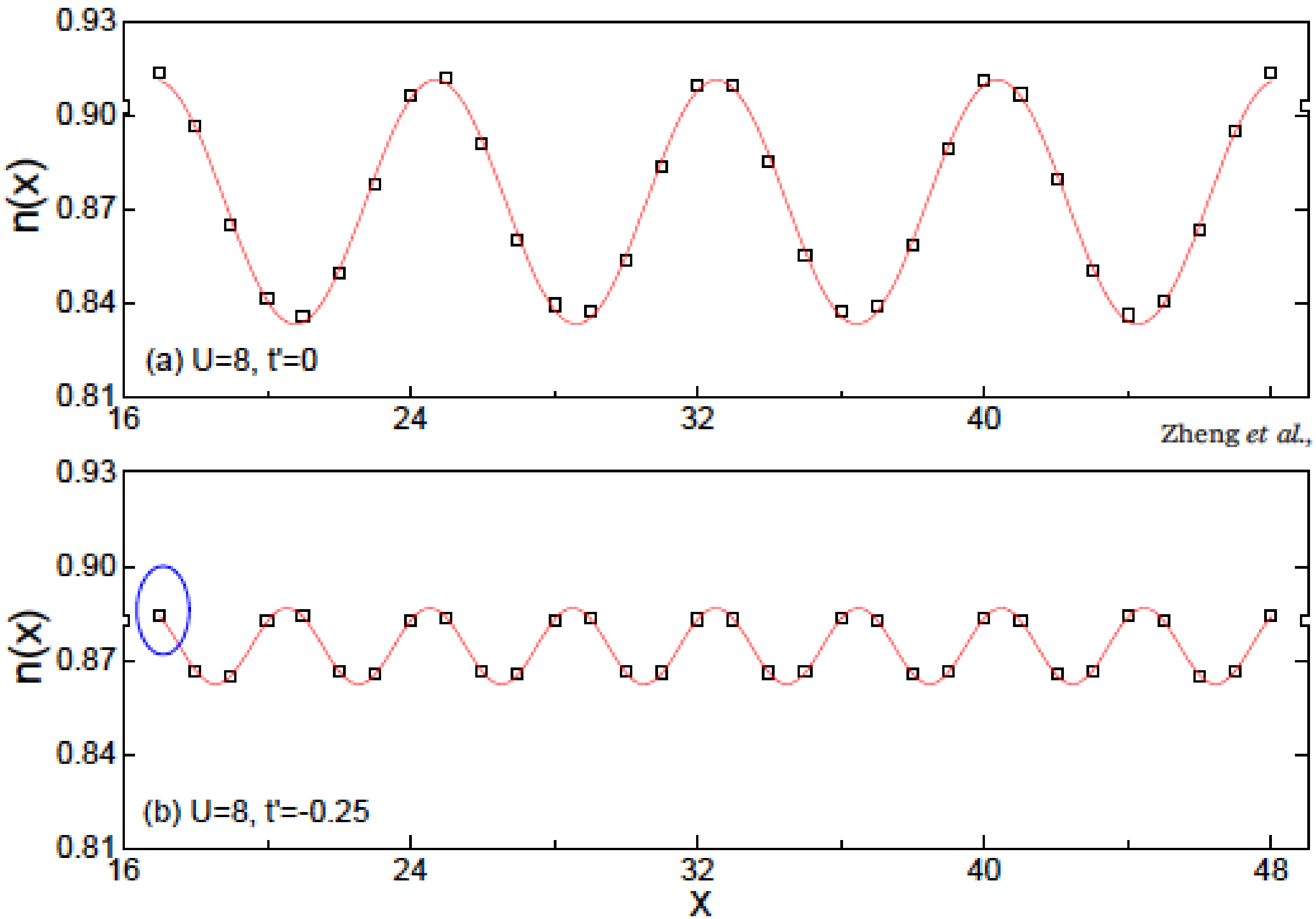

Zheng *et al.*, *Science* 358, 1155–1160 (2017)

$\lambda=1/\delta$

- Filled stripes
- Large amplitude
- Same as Zheng et al.

$\lambda=1/2\delta$

- Half-filled stripes
- Smaller amplitude

CDW & spin correlations: ½ filled stripes

$$U = 12t, \qquad t' = -0.25t$$

$$\delta = \frac{1}{10}, \frac{1}{12}$$

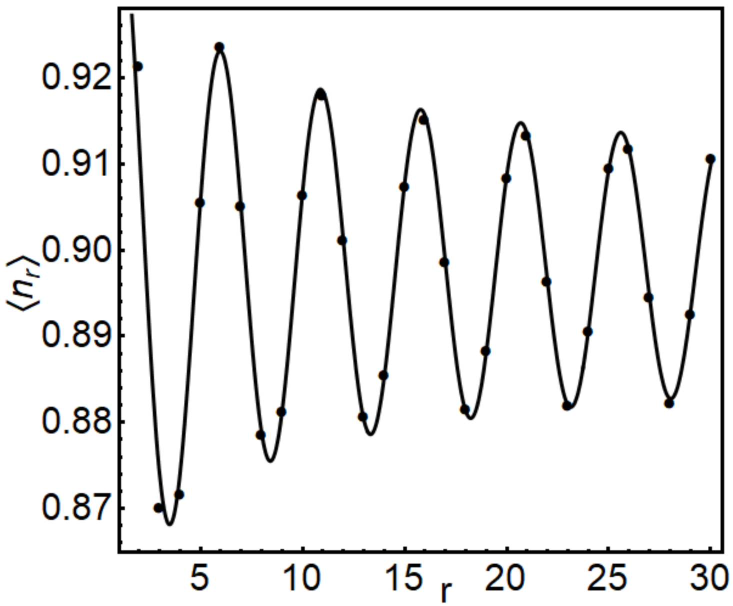

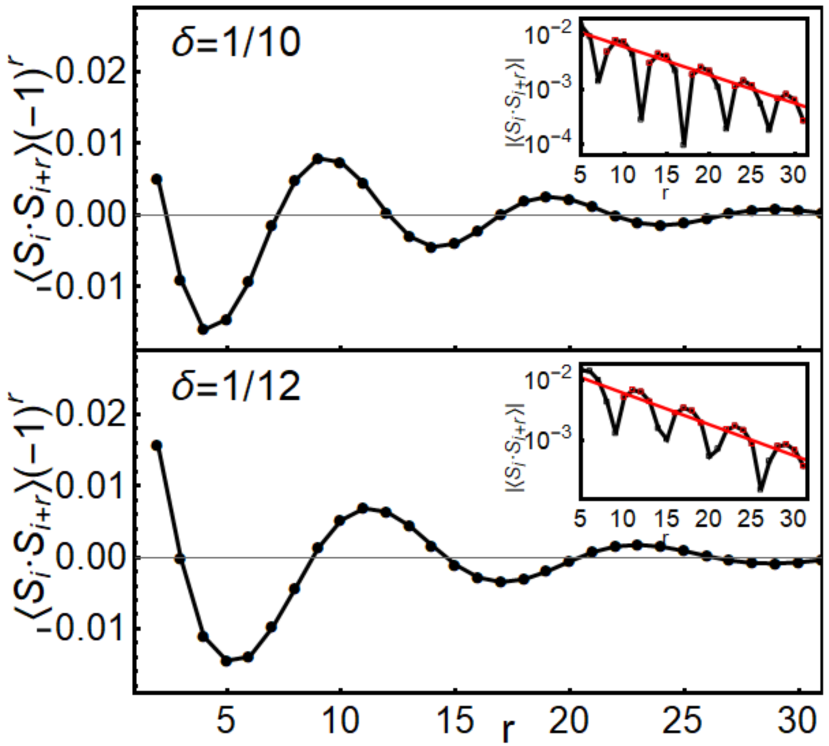

wavelength $\lambda = \frac{1}{2\delta}$ half hole per unit cell

Quasi-long-range CDW

$$n(r) = n_0 + \delta n \cos(2k_F r + \phi)\, r^{-K_C/2}$$

S.R. White *et al.*, PRB **65**, 165122 (2002)

wavelength $\lambda = \frac{1}{\delta}$

Exponential decay $|F(r)| \propto e^{-r/\xi_s}$ with $\xi_s \sim 8.5$ for $\delta = 1/10$, $\xi_s \sim 8.3$ for $\delta = 1/12$

Superconducting correlations: ½ filled stripes

Pair field correlator

$$\Phi_{\alpha\beta}(r) = \frac{1}{L_y}\sum_y \langle \Delta_\alpha^\dagger(x_0, y)\Delta_\beta(x_0 + r, y)\rangle$$

$$\Delta_\alpha^\dagger(x,y) = \frac{1}{\sqrt{2}}\left(c^\dagger_{(x,y),\uparrow}c^\dagger_{(x,y)+\alpha,\downarrow} - c^\dagger_{(x,y),\downarrow}c^\dagger_{(x,y)+\alpha,\uparrow}\right)$$

t-J (t'=0)

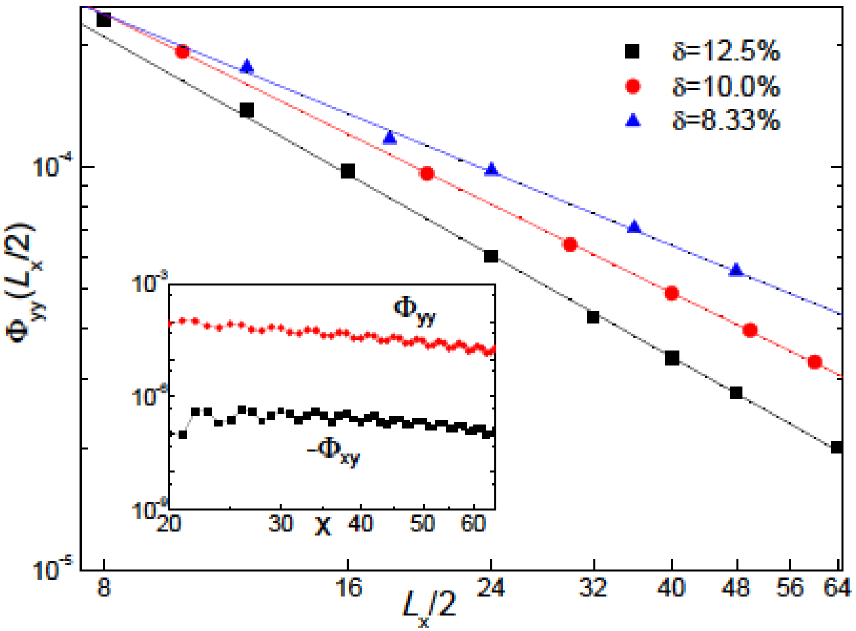

d-wave SC ($\Phi_{yy} > 0, \Phi_{xy} < 0$)

Hubbard (t'=-0.25t)

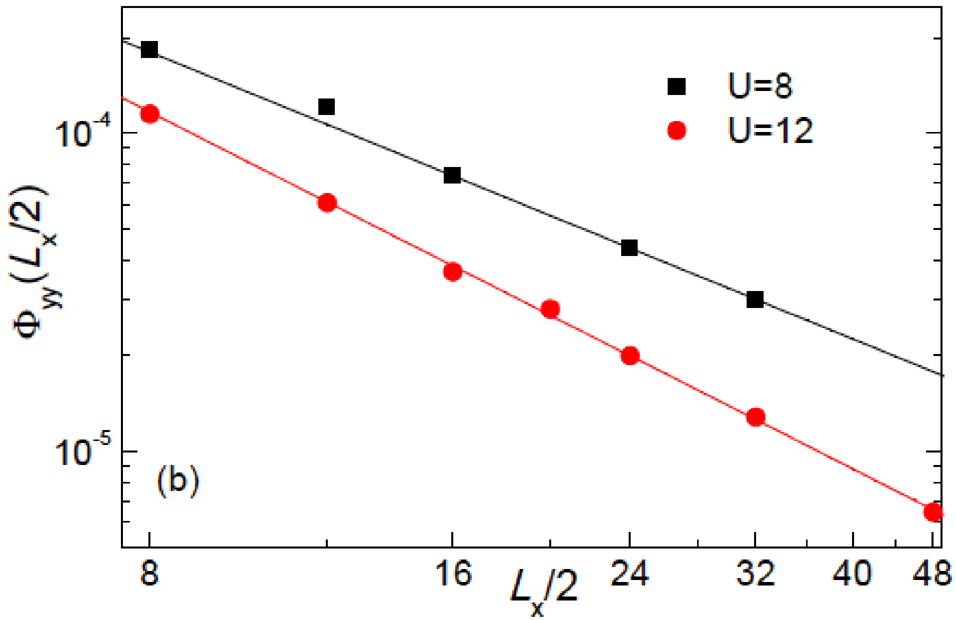

Power-law decay

$$\Phi_{\alpha\beta}(x) \propto |x|^{-K_{sc}}$$

Luther-Emery liquid: exponents & central charge

$U = 12t$

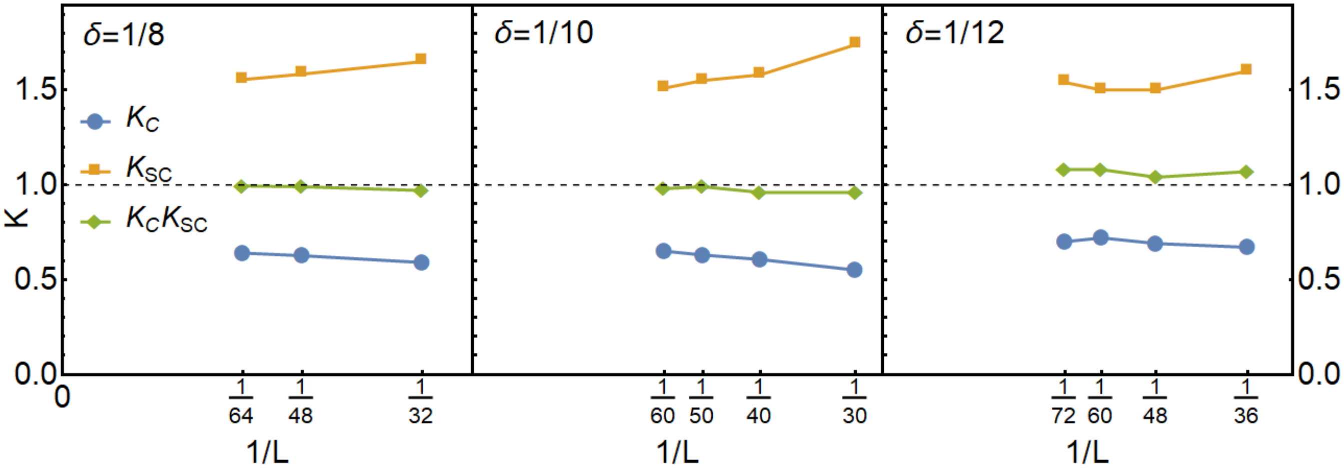

Entanglement Entropy:

$S = -\mathrm{Tr}\rho \ln \rho$

$S(l) = \frac{c}{6} \ln l + \tilde{c}$

$c \sim 1.04$ for $\delta = \frac{1}{12} \sim \frac{1}{8}$

- Power law decay CDW and SC correlation with exponent K_C and K_{SC}
- Luther Emery liquid: $K_C\, K_{SC} = 1$, single gapless mode

A. Luther and V. J. Emery, PRL **33**, 589 (1974)

$$S\left(\frac{L_x}{2}\right) = \frac{c}{6} \ln L_x + \tilde{c}$$

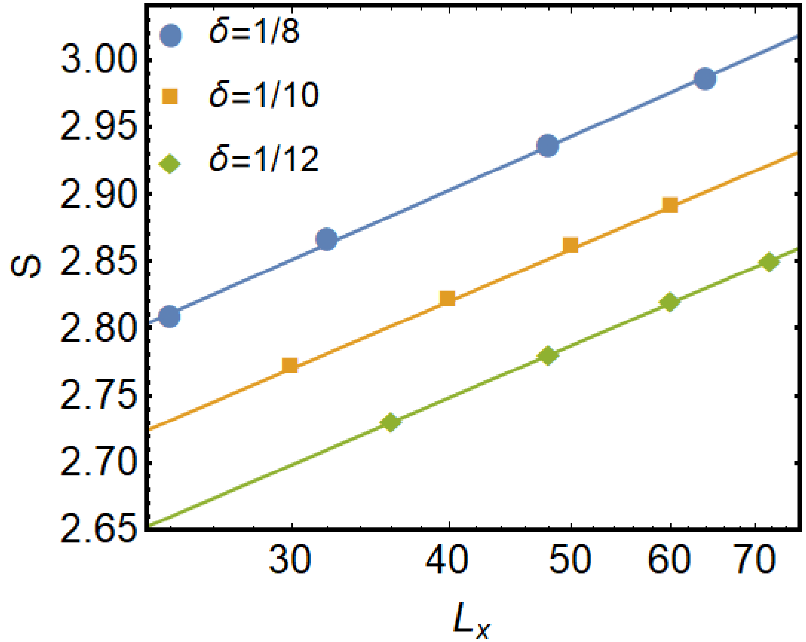

Ground state phase diagram: 4 leg ladders

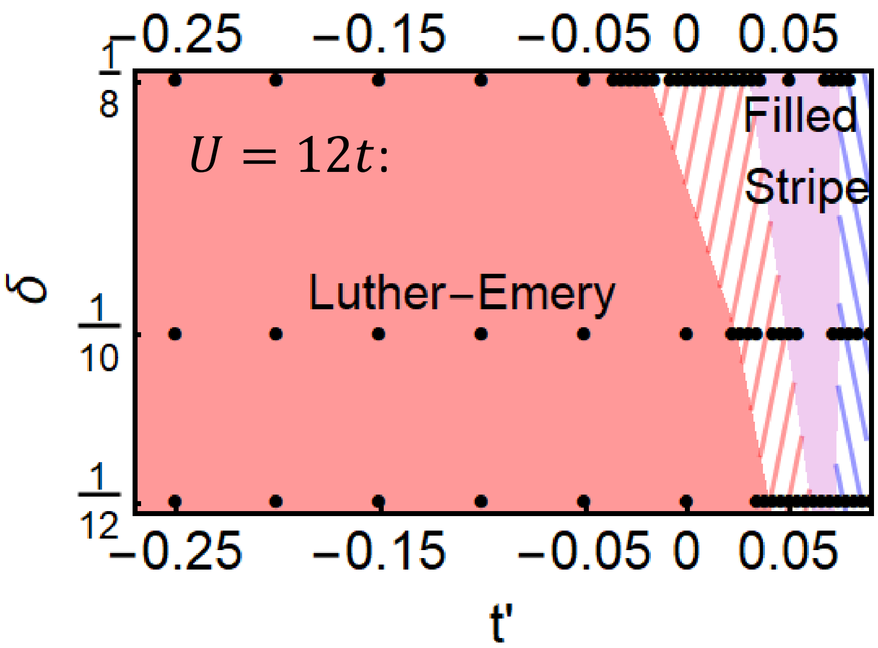

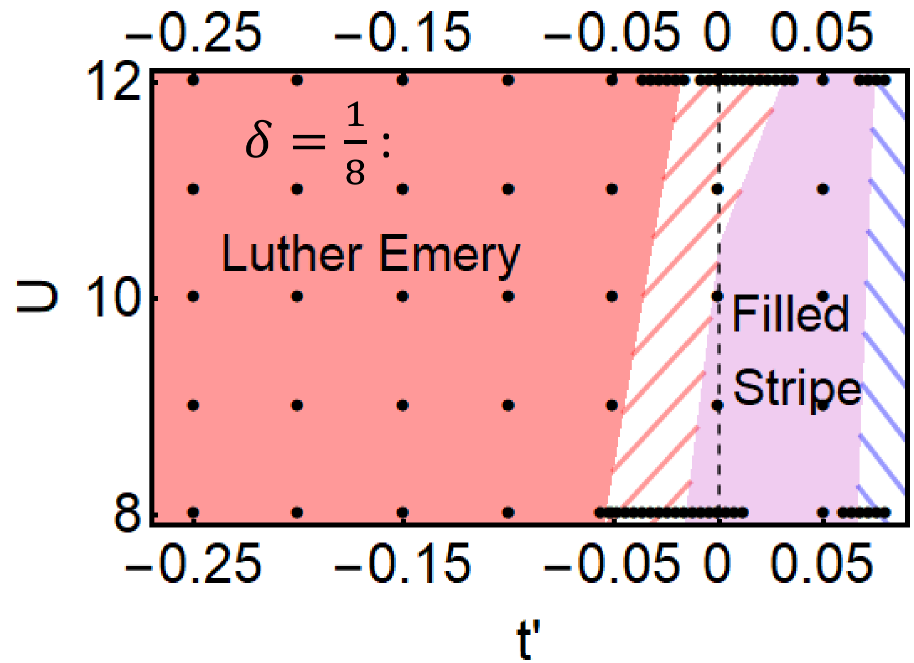

Shaded intermediate regions: phase separation / incommensurate

Filled Stripe:
- Long range CDW
- Short range pair correlations, no SC
- Spin gap

Luther-Emery:
- Quasi-long-range CDW and SC
- Spin gap

Ground state phase diagram: 4 leg ladders

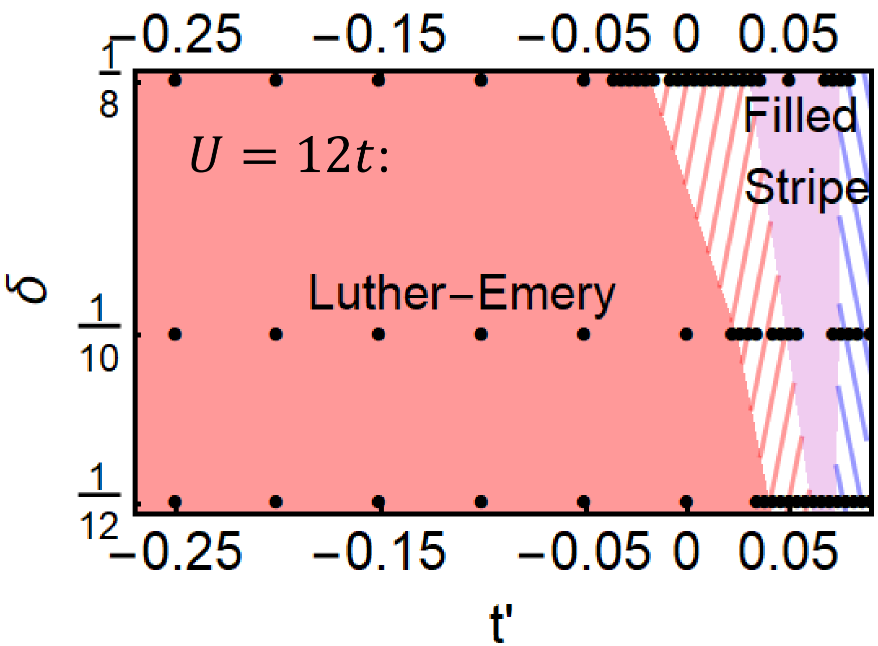

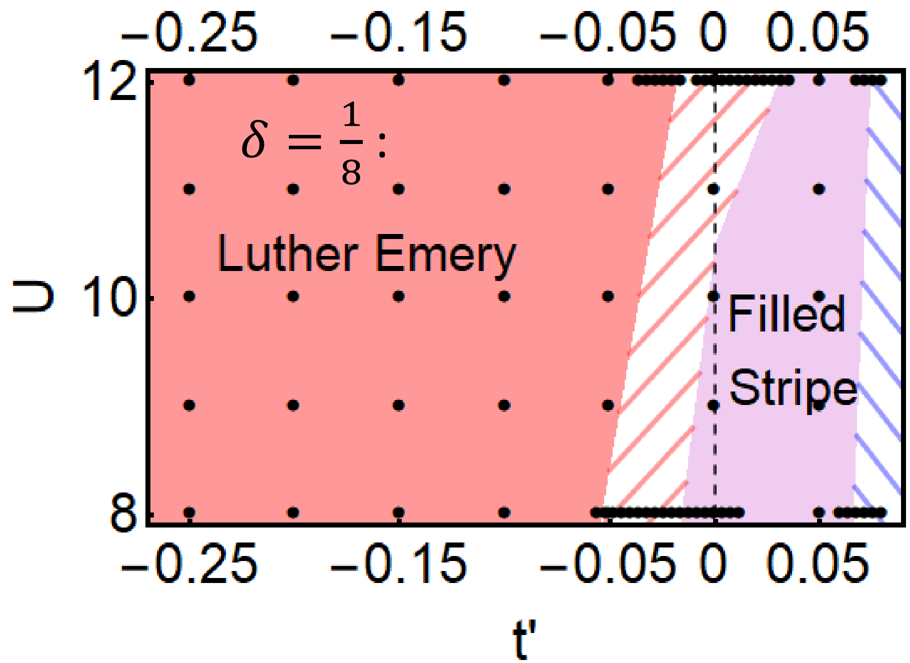

Shaded intermediate regions: phase separation / incommensurate

Fragile filled stripe phase, unstable when

- $U > 10t,\ t' = 0$
- $t' < -0.02t,\ U = 8t$

Introduction: Exciton Condensation

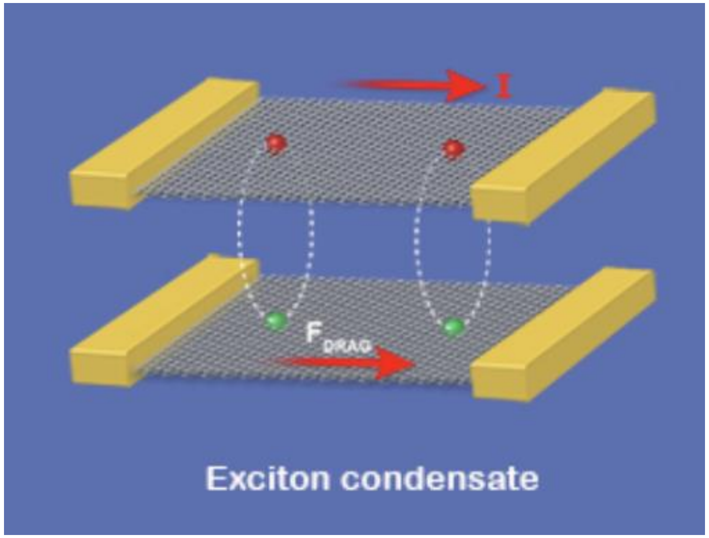

Michael S. Fuhrer, Alex R. Hamilton, *Physics* 9, 80

Exciton condensation

- Exciton can condensate like usual boson

Bilayer system with opposite doping

- Electron-hole recombination suppress the process
- One possible solution: spatially separate electrons and holes
- Bilayer systems with opposite doping are ideal for exciton condensation study

Xuxin Huang, Martin Claassen, Edwin W. Huang, Brian Moritz, Thomas P. Devereaux arXiv:1809.06439

Introduction: Model & Method

- Model: Bilayer Hubbard Model with opposite doping

$$\hat{H} = -t \sum_{\langle i,j \rangle,\alpha,\sigma} (\hat{c}^{\dagger}_{i\alpha\sigma}\hat{c}_{j\alpha\sigma} + h.c.) - \mu \sum_{i\sigma} (\hat{n}_{iA\sigma} - \hat{n}_{iB\sigma})$$
$$+ U \sum_{i\alpha} (\hat{n}_{i\alpha\uparrow} - \frac{1}{2})(\hat{n}_{i\alpha\downarrow} - \frac{1}{2}) + V \sum_{i\sigma\sigma'} (\hat{n}_{iA\sigma} - \frac{1}{2})(\hat{n}_{iB\sigma'} - \frac{1}{2})$$

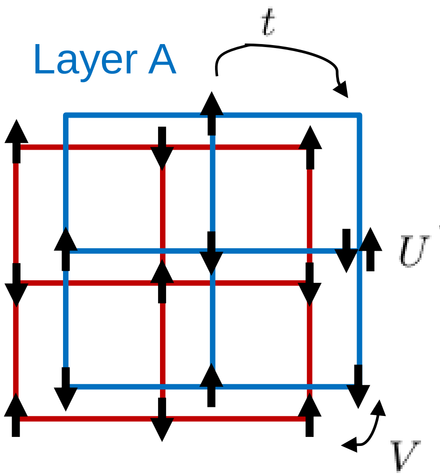

- Method: Determinant Quantum Monte Carlo (DQMC)
  - Numerically exact; finite temperatures
  - Limited by fermion sign problem

$$\langle \hat{A} \rangle = \frac{\mathrm{tr}(\hat{A}e^{-\beta\hat{H}})}{\mathrm{tr}(e^{-\beta\hat{H}})} \xrightarrow[\tilde{\rho}_{\mathbf{s}}:\ \mathrm{e}^{-\beta\hat{H}} \propto \sum_{\{\mathbf{s}\}} \tilde{\rho}_{\mathbf{s}}]{\text{Hubbard-Stratonovich (HS) transformation}} \langle \hat{A} \rangle = \frac{\sum_{\{\mathbf{s}\}} \mathrm{tr}(\hat{A}\tilde{\rho}_{\mathbf{s}})}{\sum_{\{\mathbf{s}\}} \mathrm{tr}(\tilde{\rho}_{\mathbf{s}})} = \frac{\sum_{\{\mathbf{s}\}} \langle \hat{A} \rangle_{\mathbf{s}} w_{\mathbf{s}}}{\sum_{\{\mathbf{s}\}} w_{\mathbf{s}}}$$

  - Weight factor $w_{\mathbf{s}} = \det\left[\hat{I} + \hat{B}_{\mathbf{s}}\right]$ can be negative or even complex for a specific HS field configuration

Sign Problem: "Solution"

Strategy

- Sign-free if $\hat{I}+\hat{B}_{\mathbf{s}}$ has an anti-unitary symmetry $\hat{T}$, i.e.

$$\hat{T}^2=-\hat{I} \quad \text{and} \quad \hat{T}^{-1}\left(\hat{I}+\hat{B}_{\mathbf{s}}\right)\hat{T}=\left(\hat{I}+\hat{B}_{\mathbf{s}}\right)$$

- Consider an unconventional anti-unitary symmetry

$$\hat{T}=\sum_{i\sigma}[|i,A,\sigma\rangle\langle i,B,\sigma|-|i,B,\sigma\rangle\langle i,A,\sigma|]\hat{K}$$

Proof of sign-free regime

- Change variables: $\hat{N}_i=\sum_{\sigma}[\hat{n}_{iA\sigma}+\hat{n}_{iB\sigma}]$ $\hat{M}_i=\sum_{\sigma}[\hat{n}_{iA\sigma}-\hat{n}_{iB\sigma}]$
- Continuous HS transformation; introduce HS fields $\{s_{Nil},s_{Mil}\}$

$$\hat{I}+\hat{B}_{\mathbf{s}}=\hat{I}+\prod_l e^{-\Delta\tau\hat{h}_0}e^{2\sum_i s_{Nil}\sqrt{-\Delta\tau\frac{U-V}{4}}\hat{N}_i}e^{2\sum_i s_{Mil}\sqrt{-\Delta\tau\frac{U+V}{4}}\hat{M}_i}$$

$$\hat{T}^{-1}\sqrt{-\beta\frac{U-V}{4}}\hat{N}\hat{T}=\left[\sqrt{-\beta\frac{U-V}{4}}\right]^*\hat{N}$$

$$\hat{T}^{-1}\sqrt{-\beta\frac{U+V}{4}}\hat{M}\hat{T}=-\left[\sqrt{-\beta\frac{U+V}{4}}\right]^*\hat{M}$$

- No sign problem in the parameter regime $|U|\leq V$

Results: SU(4) symmetry point

Measurements

- Excitonic correlation function:

$$\langle \hat{b}^\dagger_{\vec{q}} \hat{b}_{\vec{q}} \rangle,\ \hat{b}^\dagger_{\vec{q}} = \sum_{\vec{k}\sigma\sigma'} \hat{c}^\dagger_{\vec{k}+\vec{q}A\sigma} \hat{c}_{\vec{k}B\sigma'}$$

- Biexcitonic correlation function:

$$P_e(\vec{q}) = \frac{1}{L^2} \sum_{\vec{R},\vec{r}} e^{-i\vec{q}\cdot\vec{R}} \langle \Delta^\dagger(\vec{R}+\vec{r}) \Delta(\vec{r}) \rangle$$

$$\Delta(\vec{r}) = \hat{c}^\dagger_{\vec{r}B\uparrow} \hat{c}^\dagger_{\vec{r}B\downarrow} \hat{c}_{\vec{r}A\downarrow} \hat{c}_{\vec{r}A\uparrow}$$

- Electron doped layer spin correlation function:

$$S_c(\vec{q}) = \frac{1}{L^2} \sum_{\vec{R},\vec{r}} e^{-i\vec{q}\cdot\vec{R}} \langle (\hat{n}_{\vec{R}+\vec{r}A\uparrow} + \hat{n}_{\vec{R}+\vec{r}A\downarrow})(\hat{n}_{\vec{r}A\uparrow} + \hat{n}_{\vec{r}A\downarrow}) \rangle$$

- Electron doped layer charge correlation function:

$$S_s(\vec{q}) = \frac{1}{L^2} \sum_{\vec{R},\vec{r}} e^{-i\vec{q}\cdot\vec{R}} \langle (\hat{n}_{\vec{R}+\vec{r}A\uparrow} - \hat{n}_{\vec{R}+\vec{r}A\downarrow})(\hat{n}_{\vec{r}A\uparrow} - \hat{n}_{\vec{r}A\downarrow}) \rangle$$

SU(4) symmetry point

- The Hamiltonian has a SU(4) symmetry at U=V=5t, μ=0t, where it is invariant under:

$$\hat{Q} : \downarrow A \longrightarrow \uparrow B$$
$$\uparrow B \longrightarrow \downarrow A$$
$$\hat{Q}^\dagger \hat{H} \hat{Q} = \hat{H}$$

Exc corr: $\sum \hat{c}^\dagger_{k+q\uparrow A} \hat{c}_{k\uparrow B} \hat{c}^\dagger_{k'-q\uparrow B} \hat{c}_{k'\uparrow A}$

$\hat{Q}$ ↓

Spin corr: $\sum \hat{c}^\dagger_{k+q\downarrow A} \hat{c}_{k\uparrow A} \hat{c}^\dagger_{k'-q\uparrow A} \hat{c}_{k'\downarrow A}$

Results: SU(4) symmetry point

SU(4) symmetry point

- At the SU(4) symmetry point, the spin correlation function is equivalent to the excitonic correlation function

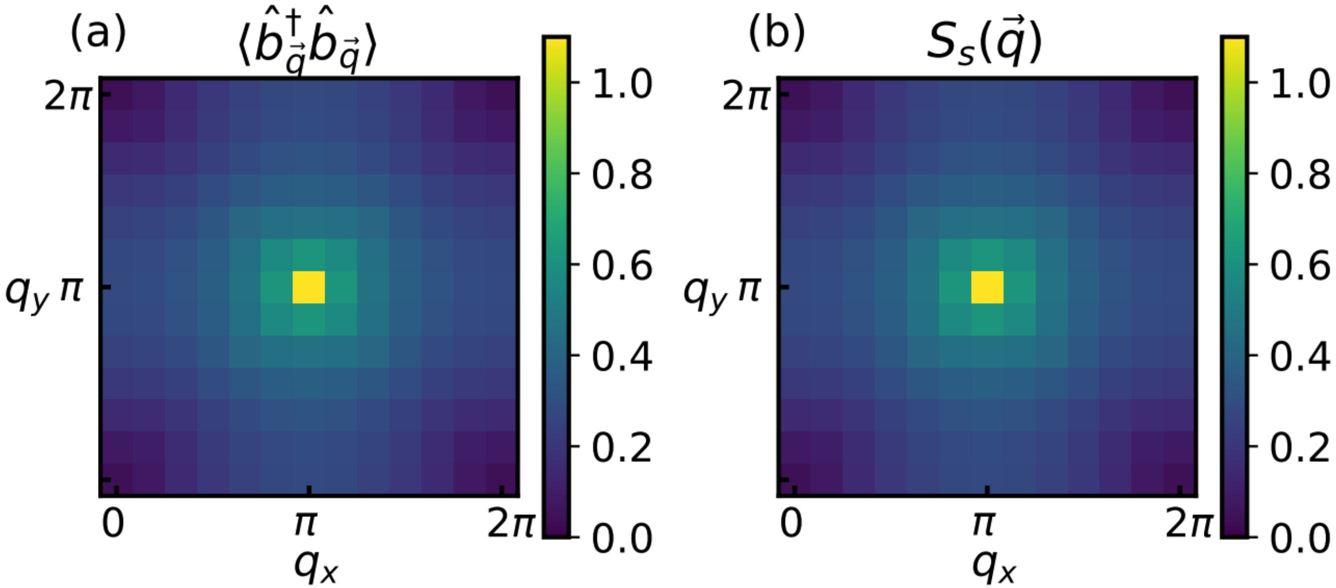

Results: Search for excitonic condensate

- Exciton condensation may be obtained by breaking the U(1) symmetry for the conserved charge $\sum_{i\sigma} \hat{n}_{iA\sigma} - \hat{n}_{iB\sigma}$.

- Due to Mermin-Wagner theorem, such symmetry cannot be broken at finite temperature. But it remains possible to achieve quasi-long-range order by a BKT transition.

- We need an order parameter breaks the excitonic U(1) symmetry but preserves other symmetries of the Hamiltonian.
  - › Study parameter regime without the SU(4) symmetry
  - › Study the biexciton condensation order instead of the exciton condensation order

Exciton: $\hat{b}^\dagger_{\vec{q}} = \sum_{\vec{k}\sigma\sigma'} \hat{c}^\dagger_{\vec{k}+\vec{q}A\sigma} \hat{c}_{\vec{k}B\sigma'}$

Biexciton: $\Delta(\vec{r}) = \hat{c}^\dagger_{\vec{r}B\uparrow} \hat{c}^\dagger_{\vec{r}B\downarrow} \hat{c}_{\vec{r}A\downarrow} \hat{c}_{\vec{r}A\uparrow}$

Results: Away from SU(4)

- U=5t, V=6t, μ=0t-1.4t
- CDW: charge density wave
- Bi-EC: biexciton condensation
- BI: band insulator

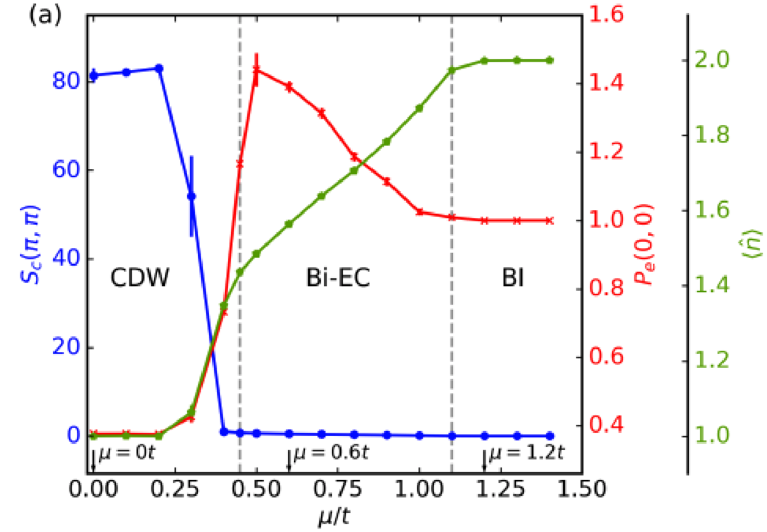

Biexcitonic correlation function

Charge correlation function

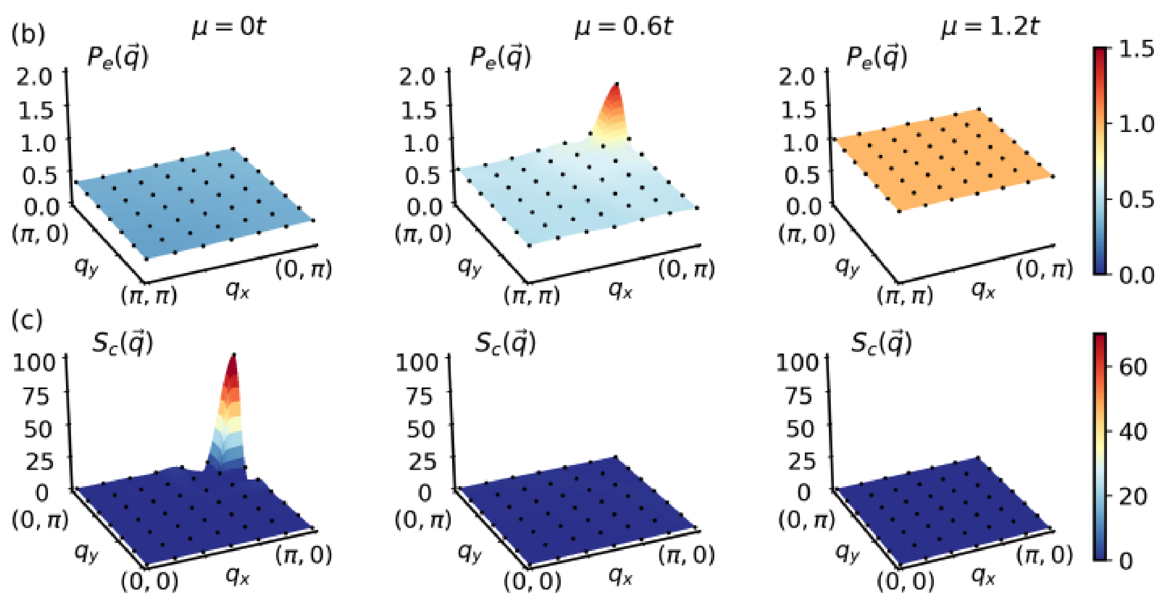

Results:

Superfluid density

- Superfluid density ρ_s can be calculated from current-current correlators measured in DQMC.
- Superfluid density and biexciton correlation function have similar behaviors

$$\rho_s = \frac{1}{16}(\delta\Lambda_{AA}^{xx} + \delta\Lambda_{BB}^{xx} - 2\delta\Lambda_{AB}^{xx}),$$

$$\delta\Lambda_{\alpha\gamma}^{xx} = \lim_{q_x\to 0}\Lambda_{\alpha\gamma}^{xx}(q_x, q_y = 0, \omega_n = 0) - \lim_{q_y\to 0}\Lambda_{\alpha\gamma}^{xx}(q_x = 0, q_y, \omega_n = 0),$$

$$\Lambda_{\alpha\gamma}^{xx}(\vec{q}, \omega_n) = \sum_{\vec{r}}\int_0^\beta d\tau e^{-i\vec{q}\cdot\vec{r}} e^{i\omega_n\tau}\Lambda_{\alpha\gamma}^{xx}(\vec{r}, \tau),$$

$$\Lambda_{\alpha\gamma}^{xx}(\vec{r}, \tau) = \sum_{\sigma,\sigma'}\langle\hat{j}_{\alpha,\sigma}^{x}(\vec{r}, \tau)\hat{j}_{\gamma,\sigma'}^{x}(0, 0)\rangle.$$

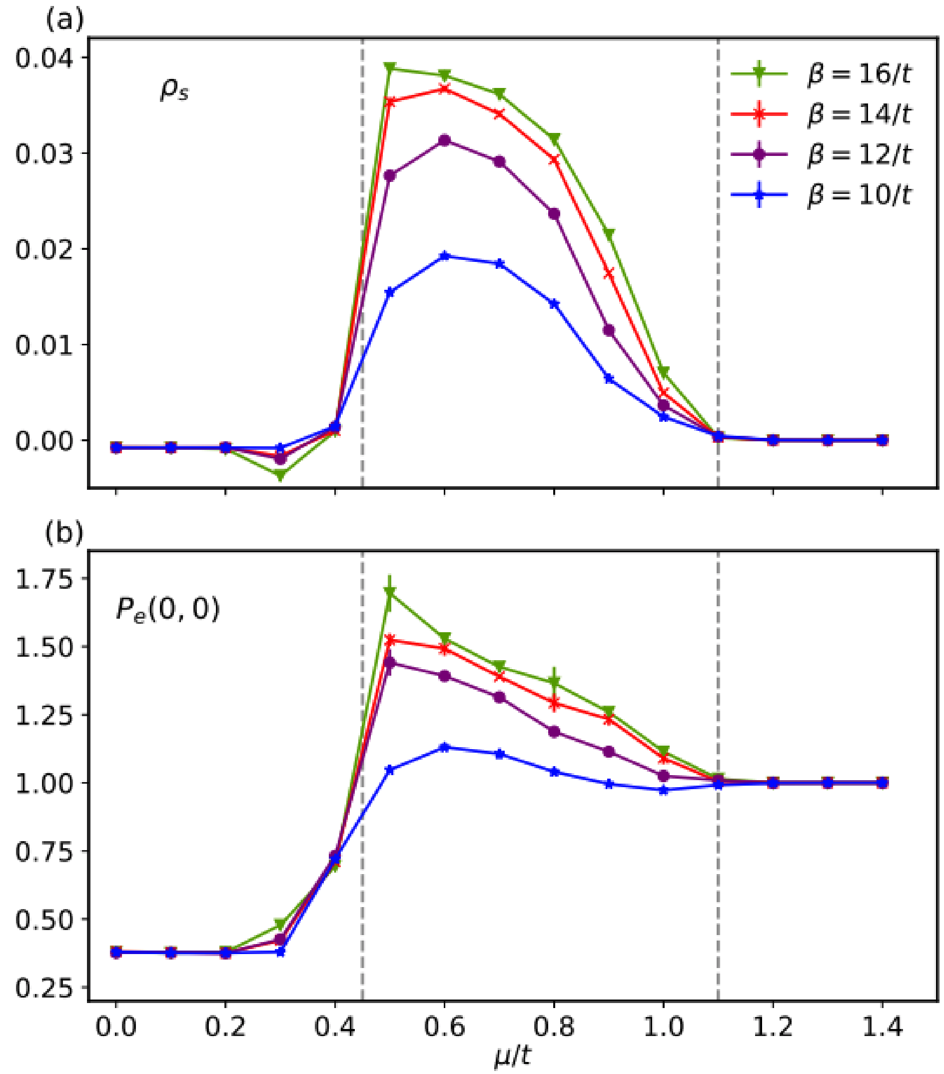

Results:

Determine transition temperature (for U=5t, V=6t and μ=0.5t)

- Method 1: universal jump of superfluid density
  - Approach from below T_c , the following relation is satisfied:

$$T_c = \frac{\pi}{2}\rho_s$$

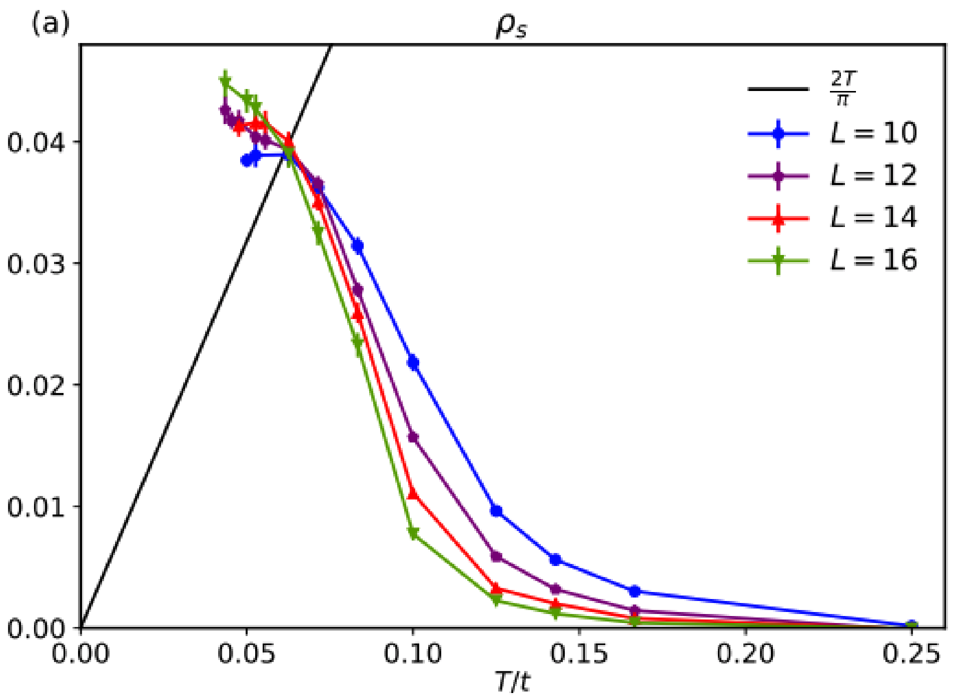

T_c ~ 0.06t

Results:

Determine transition temperature (for U=5t, V=6t and μ=0.5t)

- Method 2: finite size analysis of correlation function

$$P_e(0,0) = L^{2-\eta(T_c)} f(L/\xi), \;\; \xi \sim \exp\left[\frac{A}{(T-T_c)^{1/2}}\right].$$

$$P_e^0 = P_e(0,0) - \frac{1}{L^2}\sum_{\vec{r}}\langle\hat{\Delta}^\dagger(\vec{r})\hat{\Delta}(\vec{r})\rangle$$

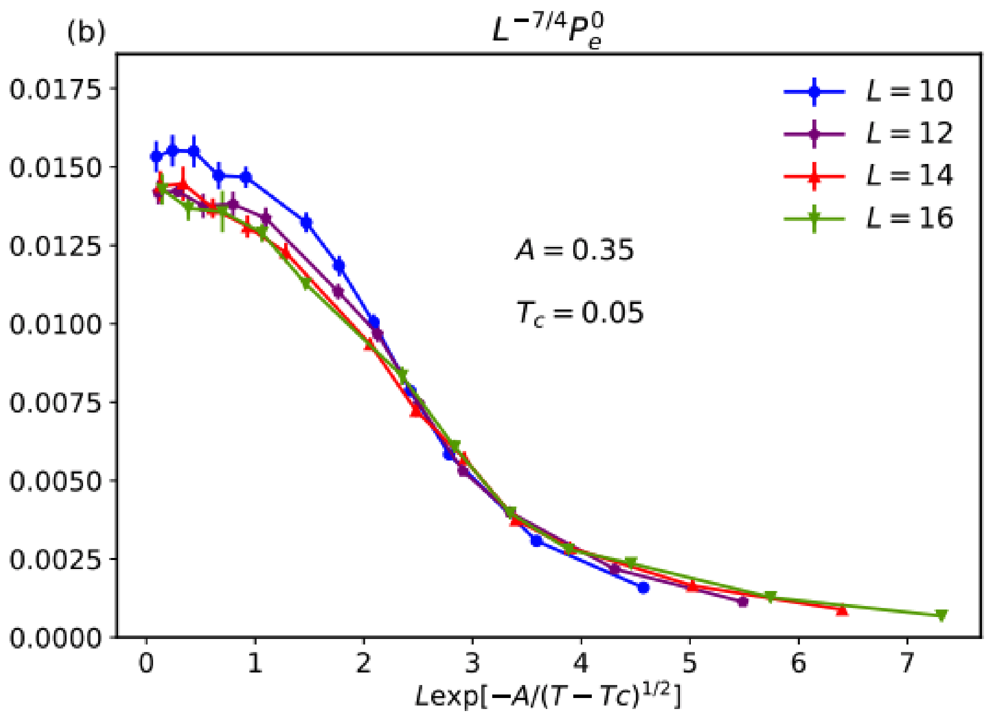

T_c ~ 0.05t

Summary

- A sign-problem-free DQMC algorithm to study bilayer Hubbard model with equal but opposite doping in the two layers in the parameter regime $|U| \leq V$.
- Away from SU(4) point, we find convincing numerical evidence for a biexcitonic condensate, which competes with (π, π) charge order at finite electron-hole doping.
- We have extracted the BKT transition temperature by two independent approaches, with an estimate for $T_c \sim 0.05t\text{-}0.06t$.

Xuxin Huang, Martin Claassen, Edwin W. Huang, Brian Moritz, Thomas P. Devereaux

arXiv:1809.06439

Stanford University

DMRG Studies of Multi-Component Hubbard Models and Higher Spin systems

DMRG Studies of Two-Component Hubbard Models for Moire Materials

- Twisted bilayer graphene
- Trilayer graphene-boron nitride with Moire potential

Spin Liquid in Spin-One Kitaev Material

Koshino et al.(18)

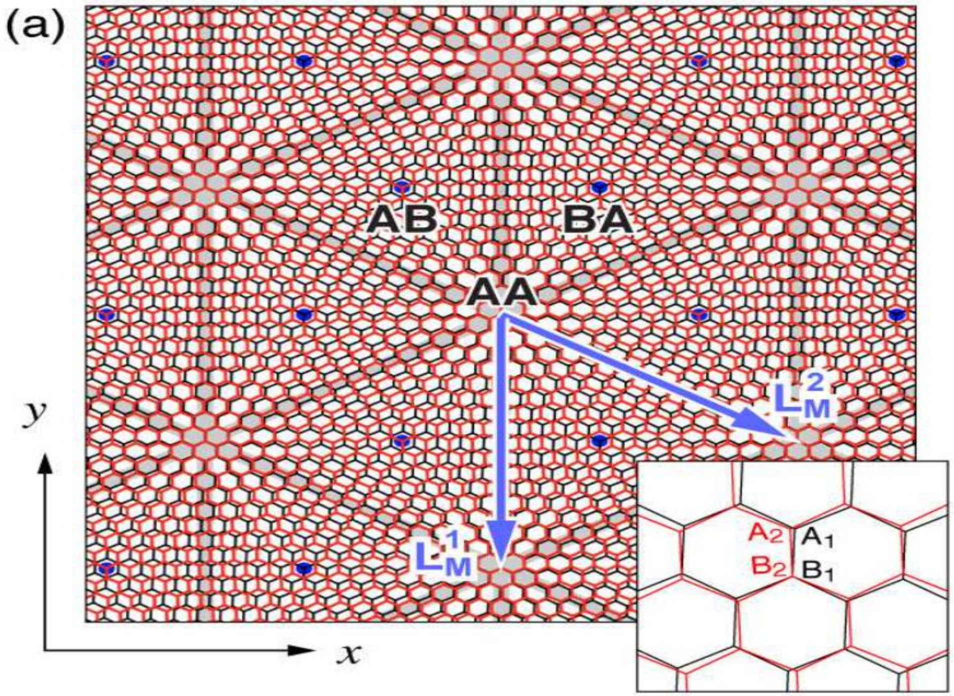

Hubbard U driven transition

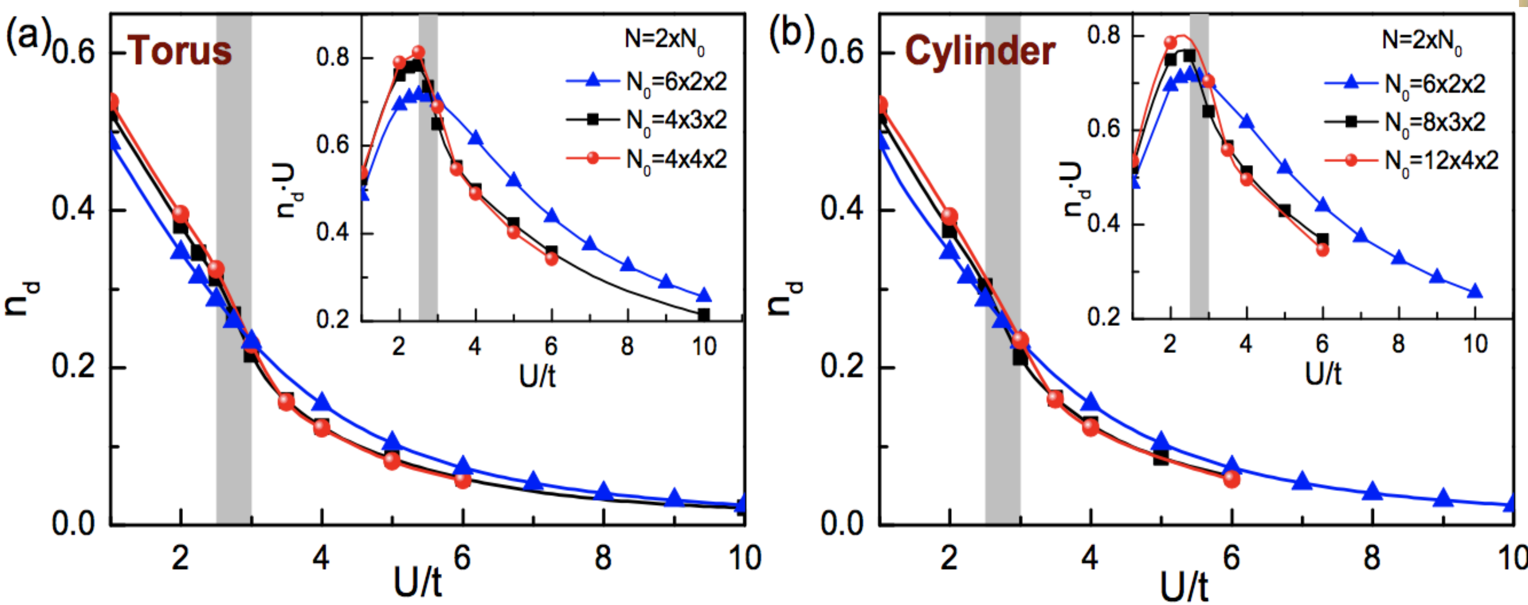

$$H = H_0 + H_{\text{int}},$$

$$H_0 = -t \sum_{\langle i,j\rangle\sigma} \sum_{\alpha=1,2} \left(c^{\dagger}_{i\sigma,\alpha} c_{j\sigma,\alpha} + h.c. \right),$$

$$H_{\text{int}} = U \sum_i \left(\sum_{\sigma,\alpha} n_{i\sigma,\alpha} - 1 \right)^2,$$

Identifying Uc ~3

We consider ¼ filling number
That is one electron per
unit cell

$$n_d = \frac{1}{N_0} \sum_{i=1}^{N_0} \left\langle \left[\sum_{\sigma,\alpha} n_{i\sigma,\alpha} - 1 \right]^2 \right\rangle,$$

Robust spin/orbital density wave

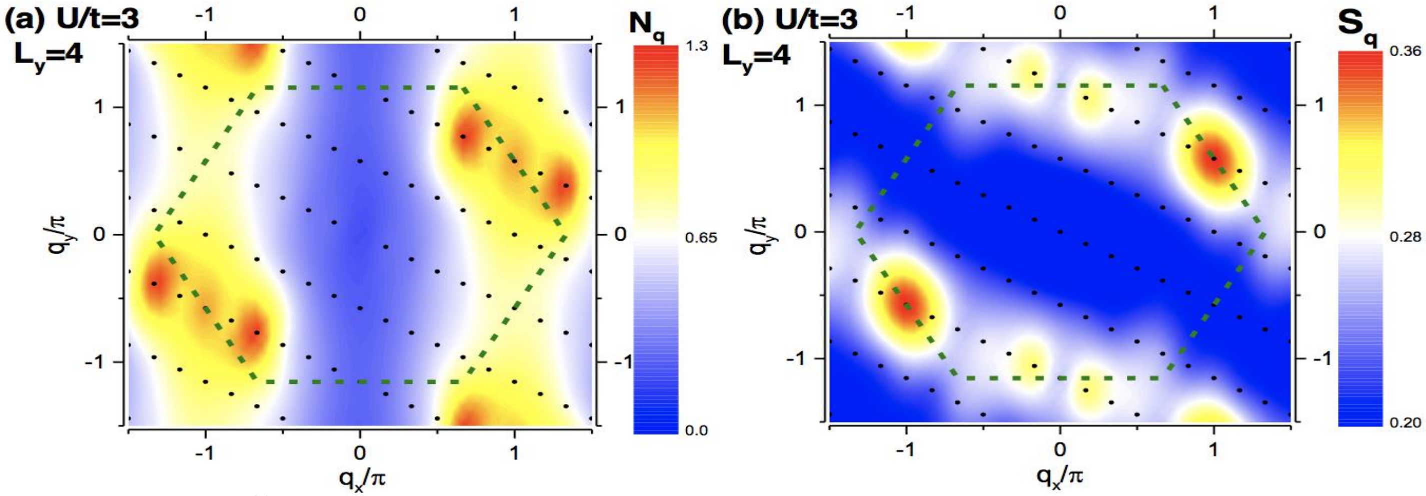

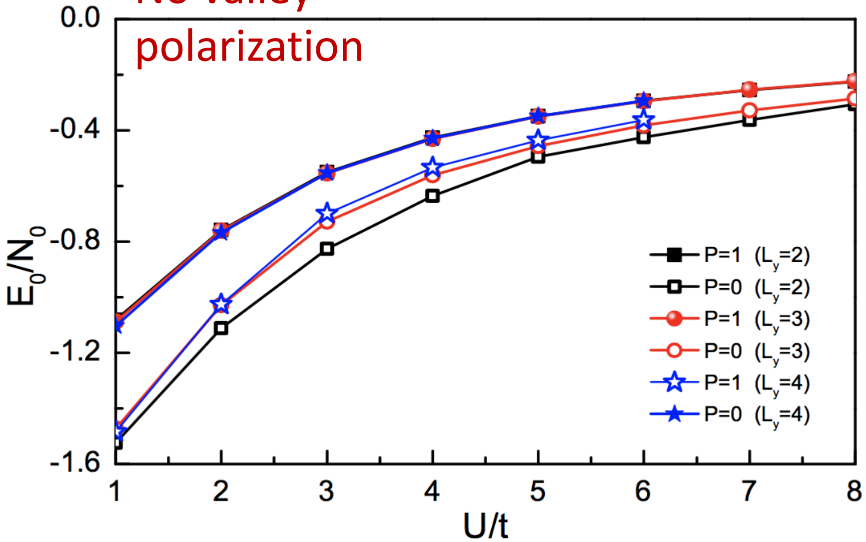

Future work will study the interplay of different lattice models and interactions, and the emergence of superconductivity In such systems.

Publications

1. **Quantum phase diagram of spin-*1* J_1-J_2 Heisenberg model on the square lattice: an infinite projected entangled-pair state and density matrix renormalization group study**, R. Haghshenas, Wang-Wei Lan, Shou-Shu Gong, D. N. Sheng, Phys. Rev. B 97, 184436 (2018).
2. **A single-layer tensor-network study of kagome Heisenberg model with chiral interactio**n, R. Haghshenas, Shou-Shu Gong, D. N. Sheng, arXiv:1812.11436, submitted to Phys. Rev. B.
3. **Single-hole wave function in two dimensions: A case study of the doped Mott insulator**, Shuai Chen, Qing-Rui Wang, Yang-Qi, D. N. Sheng, Zheng-Yu Weng, arXiv:1812.05627, submitted to Phys. Rev. B.
4. **Spin/orbital density wave and Mott insulator in two-orbital Hubbard model on honeycomb lattice**, Zheng Zhu, D. N. Sheng, Liang Fu**,** arXiv:1812.05661, submitted to Phys. Rev. Lett.
5. **Half-filled Landau levels: a continuum and sign-free regularization for 3D quantum critical points,** Matteo Ippoliti, Roger S. K. Mong, Fakher F. Assaad and Michael P. Zaletel, Phys. Rev. B 98, 235108.
6. **Observation of a chiral spin liquid phase of the Hubbard model on the triangular lattice: a density matrix renormalization group study,** Aaron Szasz, Johannes Motruk, Michael P. Zaletel, Joel E. Moore, arXiv:1808.00463.
7. **Superconductivity in the Hubbard model and its interplay with charge stripes and next-nearest hopping t',** Hong-Chen Jiang, Thomas P. Devereaux, arXiv:1806.01465 (Science accepted).
8. **Superconductivity in the doped t-J model: results for four-leg cylinders,** Hong-Chen Jiang, Zheng-Yu Weng, Steven A. Kivelson, Phys. Rev. B 98, 140505 (2018).
9. **Symmetry protected topological Luttinger liquids and the phase transition between them**, Hong-Chen Jiang, Zi-Xiang Li, Alexander Seidel, Dung-Hai Lee, Science Bulletin 63, 753 (2018).
10. **SwitchNet: a neural network model for forward and inverse scattering problems.** Yuehaw Khoo and Lexing Ying. [PDF]
11. **Convex relaxation approaches for strictly correlated density functional theory**. Yuehaw Khoo and Lexing Ying. [PDF]
12. **Electronic and phononic properties of a two-dimensional electron gas coupled to dipolar phonons via small-momentum-transfer scattering**, Zi-Xiang Li, T. P. Devereaux, & D.-H. Lee, arXiv. 1812.10262.
13. **Breakdown of Migdal-Eliashberg theory; a determinant quantum Monte Carlo study,** Ilya Esterlis, Benjamin Nosarzewski, Edwin W. Huang, Brian Moritz, Thomas P. Devereaux, Douglas J. Scalapino, Steven A. Kivelson, Phys. Rev. B **97**, 140501(R) (2018).
14. **Phases of a phenomenological model of twisted bilayer graphene**, J. F. Dodaro, S. A. Kivelson, Y. Schattner, X. Q. Sun, and C. Wang, Phys. Rev. B 98, 075154 (2018).
15. **Monte Carlo Studies of Quantum Critical Metals**, Erez Berg, Samuel Lederer, Yoni Schattner, and Simon Trebst, Annual Reviews of Condensed Matter Physics 10, 63 (2019).

People supported

Faculty & Staff salary:
TPD, Co-PI (25 % FTE)
Donna Sheng, Co-PI (1.5 months summer)
Hong-Chen Jiang, Co-PI, 71% FTE
Mike Zaletel, Co-PI (summer)

Students & Postdoc fellows:
R. Haghshenas (iPEPs)
X. Y. Dong (iPEPs)
Maxime Dupont (1D Bose glass transition in spin chains)
Cheng Peng, (DMRG Hubbard and *t*-*J* models)
Yuehaw Khoo (DFT optimizations and tensor networks)
Zi-Xiang Li (sign-free DQMC e-ph)
Yoni Shattner (sign-free DQMC nematic phases)
Xuxin Huang (student, sign-free DQMC bi-exciton condensation)
Johannes Hauschild (large scale DMRG)
Jacob Marks (student, time-dependent DMRG and tensor networks)

Thank you.

Biexciton Condensation in Electron-hole Doped Hubbard Bilayers

--A SIGN-PROBLEM-FREE QUANTUM MONTE CARLO STUDY

Xuxin Huang, Martin Claassen, Edwin W. Huang, Brian Moritz, Thomas P. Devereaux

7/17/2019

Chiral spin liquid in the triangular lattice Hubbard model

Aaron Szasz, Johannes Motruk, Michael P. Zaletel, Joel E. Moore, **arXiv:1808.00463**

Model:

$$H = -t \sum_{\langle ij \rangle \sigma} c^\dagger_{i\sigma} c_{j\sigma} + \text{H.c.} + U \sum_i n_{i\uparrow} n_{i\downarrow}$$

Lattice and boundary conditions:

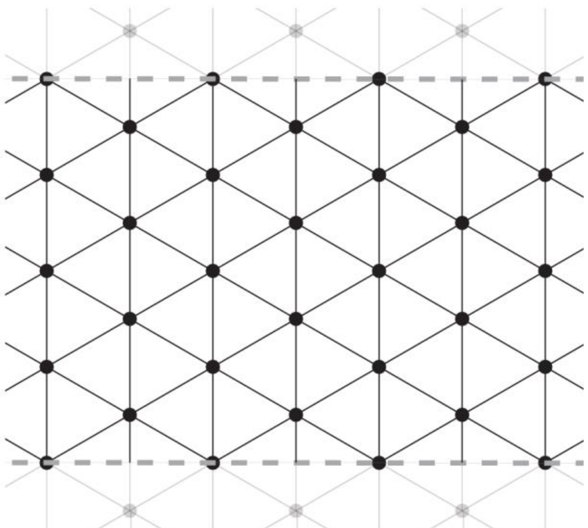

(& larger cylinders)

Find phase diagram with DMRG

- Non-magnetic insulating phase! (NMI)

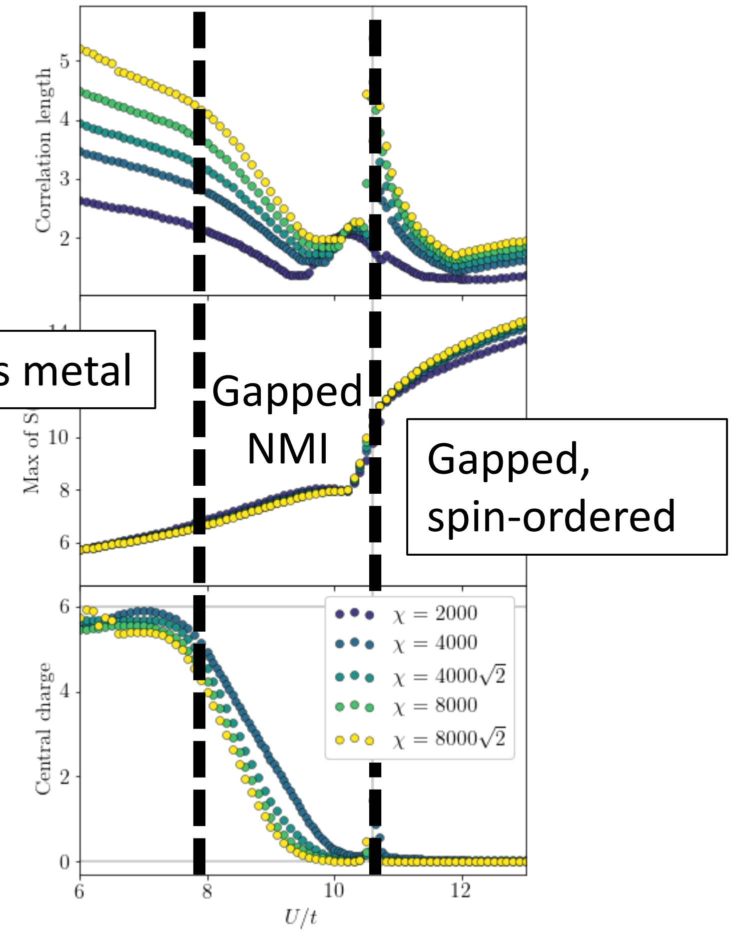

Reducing exponential complexity

4^N configurations of interacting fermions (Exponential Complexity)

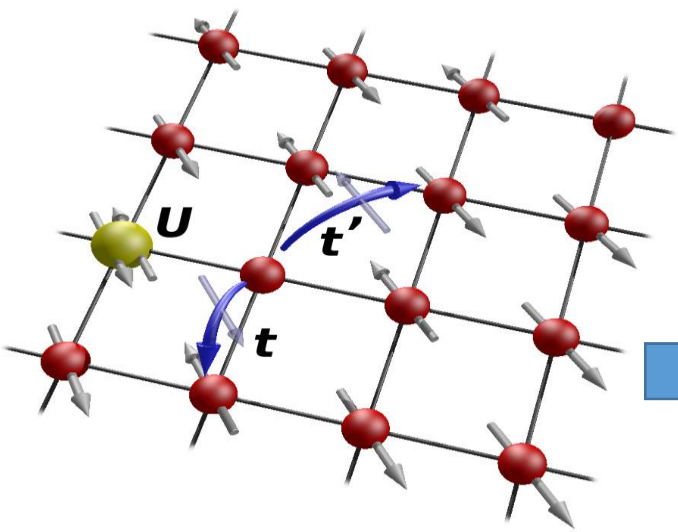

DMRG

$|\sigma\rangle$-local basis of dimension d

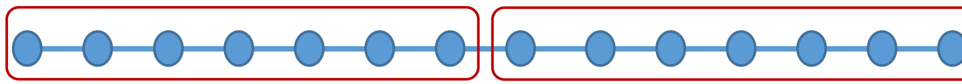

Environment (L-n site) $|j\rangle$

Ground state

$$|\psi\rangle = \sum_{ij} \psi_{ij} |i\rangle |j\rangle \quad i = 1, \ldots, d^n; \;\; j = 1, \ldots, d^{L-n}$$

Find projection operator A_n for m-important basis when d^n or d^{L-n} is too big

$$|\psi\rangle \approx \sum_{i'j'} \psi_{i'j'} |i'\rangle |j'\rangle \qquad i', j' = 1 \sim m; \;\; m \ll d^n, d^{L-n}$$

$$|i'\rangle_n = \sum_i A_n(i', i) |i\rangle_n$$

A_n=Eigenvector of reduced density matrix of m-largest eigenvalues

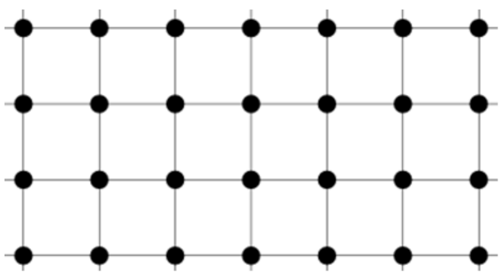

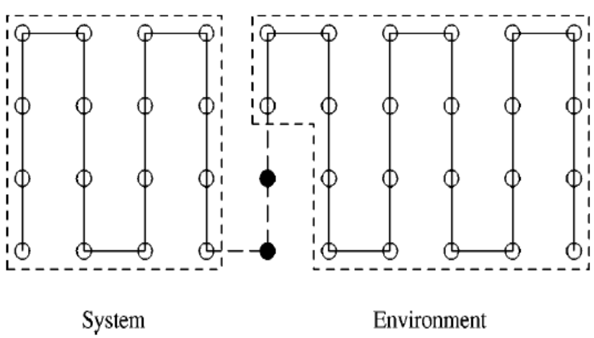

Reducing exponential complexity

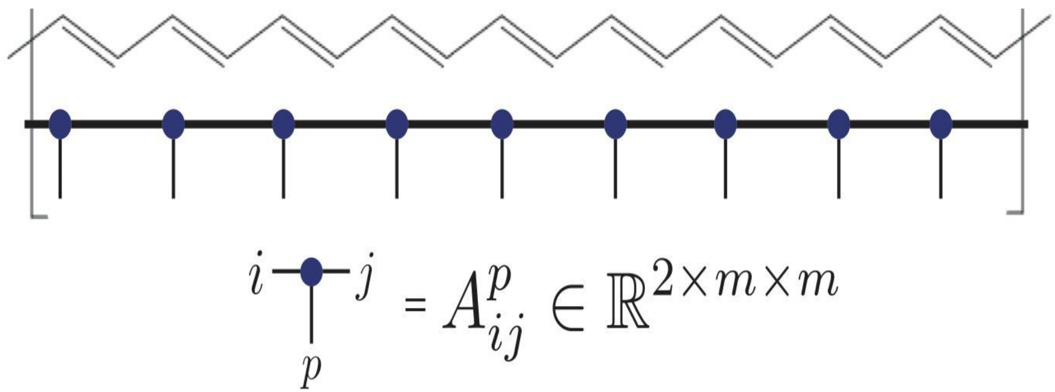

Illustration of the tensor network ansatz. The quantum state of the system is encoded by associating a tensor to each atom. In the 1D network shown here (a "matrix product state" (MPS)), the tensors are rank-3. The global state is recovered by contracting the tensors together into a network. Tensors with large dimension "*m*" can capture more strongly correlated states, but lead to higher computational costs.

SciDAC: Topological and Correlated Matter via Tensor Networks and Quantum Monte Carlo

This SciDAC proposal outlines a set of major problems in quantum materials that can be solved if large-scale implementations of tensor networks and DQMC become available. We link these problems to the major applied mathematics and computational challenges that need to be overcome. Team members previously developed important methods for long-range interactions, finite-entanglement scaling, mixed real-space and momentum-space descriptions, and tensor network skeletonization. If full Hilbert space methods can be scaled efficiently to 10^5 or more cores, many of the quantum materials problems of greatest interest become accessible. Large-scale computation then becomes a powerful means to understand experiments and differentiate between proposed theoretical scenarios.

Reducing exponential complexity

4^N configurations of interacting fermions
(Exponential Complexity)

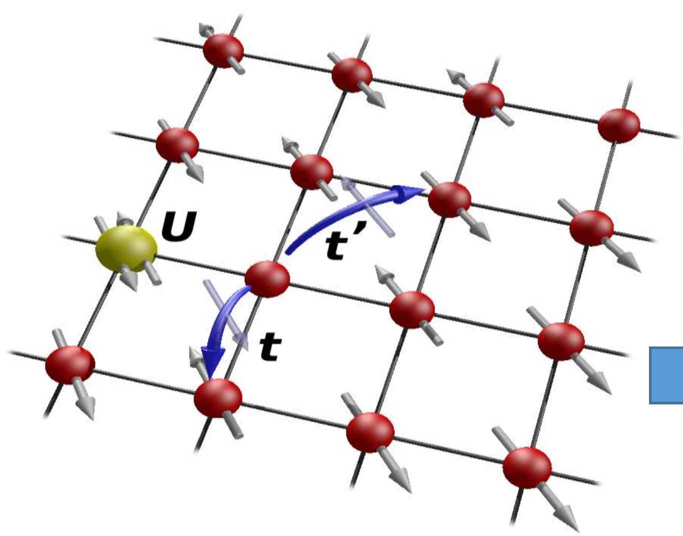

DQMC

$$Z=Tr\{e^{-\beta H}\}$$

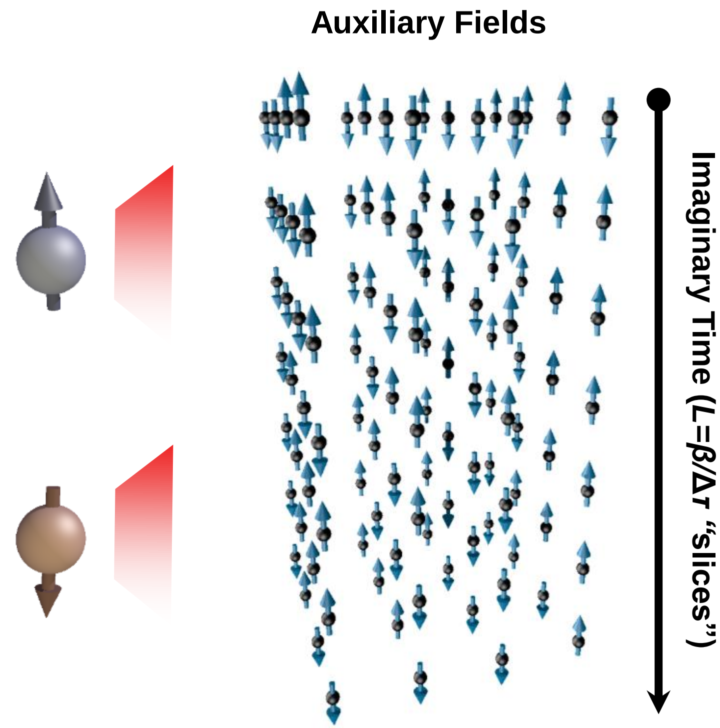

2^{NL} configurations
stochastically summed using Metropolis importance sampling

(Polynomial Complexity)

Introduction: Exciton Condensation

Exciton condensation

- Exciton can condensate like usual boson
- Exciton condensation is recently identified by momentum-resolved electron energy-loss spectroscopy(M-EELS) in the transition metal dichalcogenide semimetal 1*T*-TiSe2.

Bilayer system with opposite doping

- Electron-hole recombination suppress the process
- One possible solution: spatially separate electrons and holes
- Bilayer systems with opposite doping are ideal for exciton condensation study

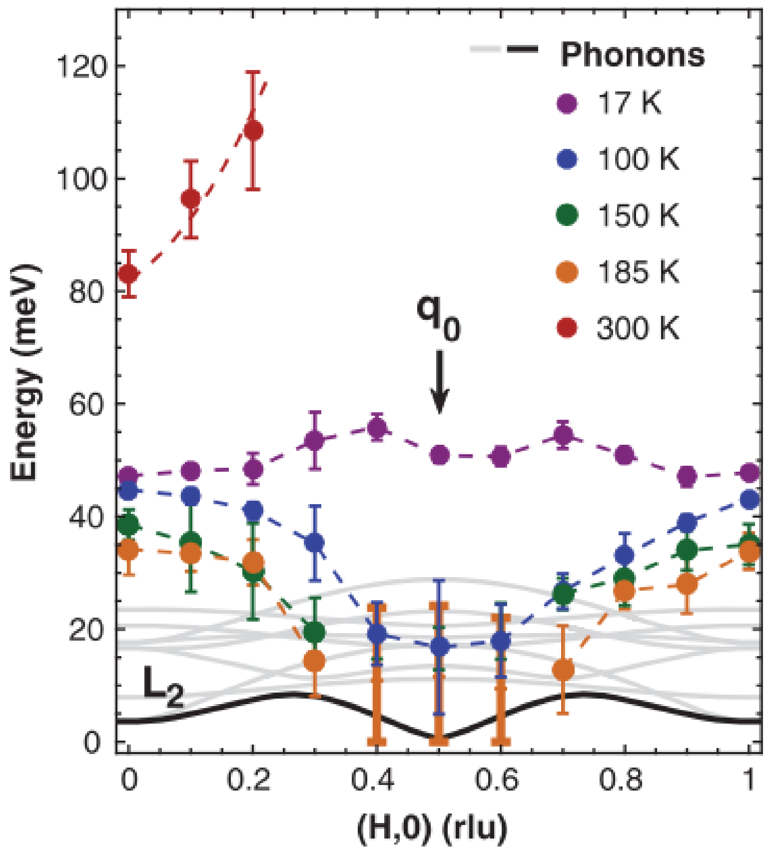

Kogar, A., Rak, M., Vig, S., Husain, A., Flicker, F., & Joe, Y. et al. (2017).

Finite size effects

t-J with π - flux

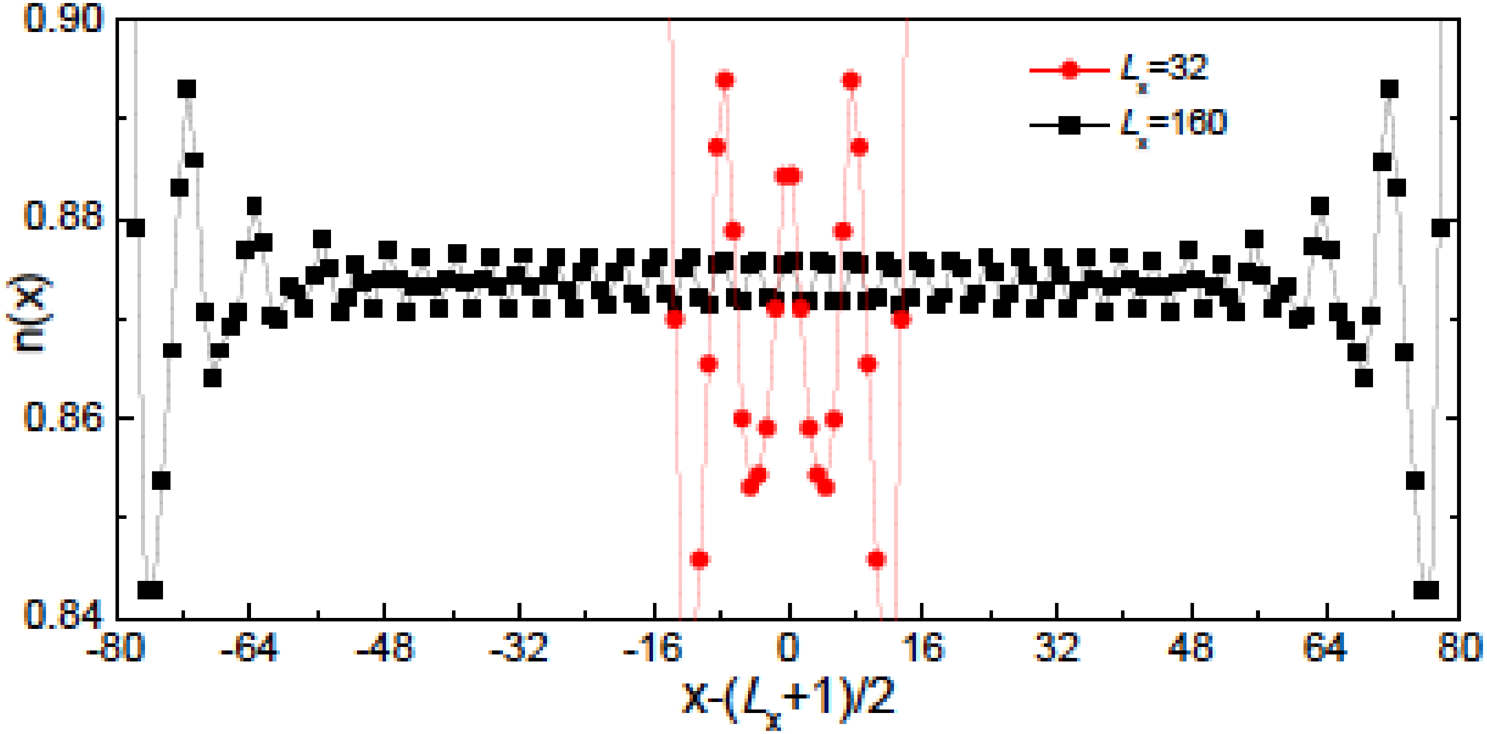

- $L_x < 48$ gives filled stripes $Q=2\pi\delta$
- $L_x = 160$ gives half filled stripes $Q=4\pi\delta$ in bulk, filled stripes at boundary

Broken *SU(2)* invariance – not converged

Magnetic moment $m_z = \frac{1}{N}\sum_{i=1}^{N} |\langle S_i^z \rangle|$

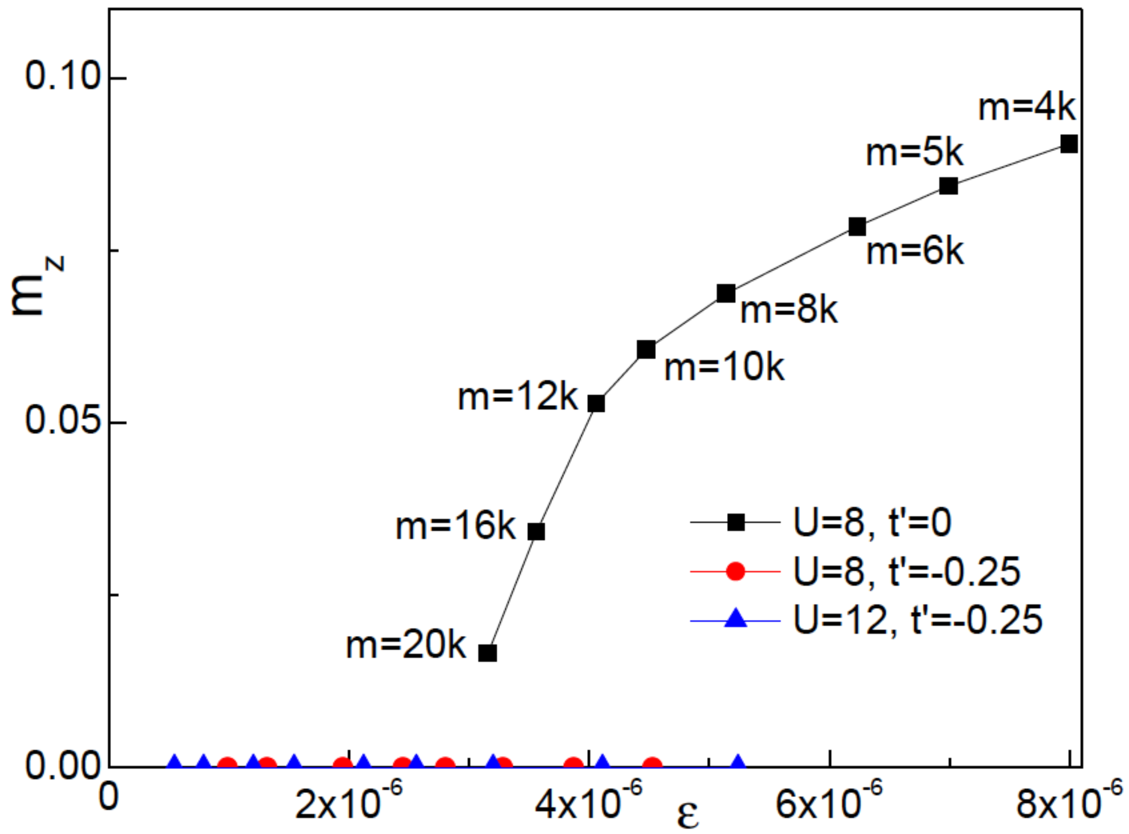

Much larger number of states are required for convergence when t'=0

Sign-free QMC

Comparisons of DMRG and QMC

Half-filled Landau levels: a continuum and sign-free regularization for 3D quantum critical points, Matteo Ippoliti, Roger S. K. Mong, Fakher F. Assaad and Michael P. Zaletel, Phys. Rev. B 98, 235108.

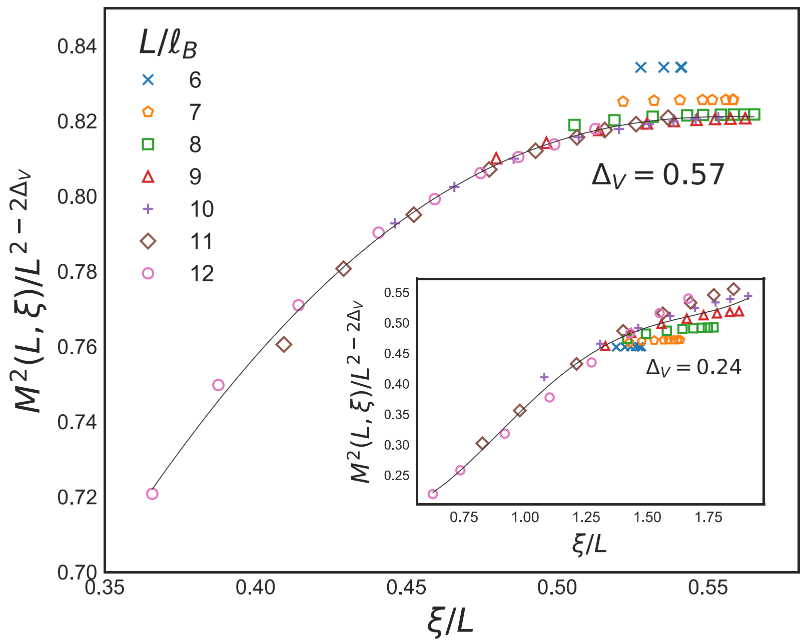

This work shows how Landau Level models can be used to implement sign-free determinantal quantum monte carlo studies of different phase transitions in frustrated magnets, such as the long studied Neel-VBS transition of the 2D Heisenberg model or the Kekule instability of monolayer graphene. Exponents of the critical point can be obtained.

Can be applied to study 2+1 dimensional conformal field theories and deconfined quantum critical points, where little is known.

Tensor Network Algorithm for Two Dimensional Spin Systems

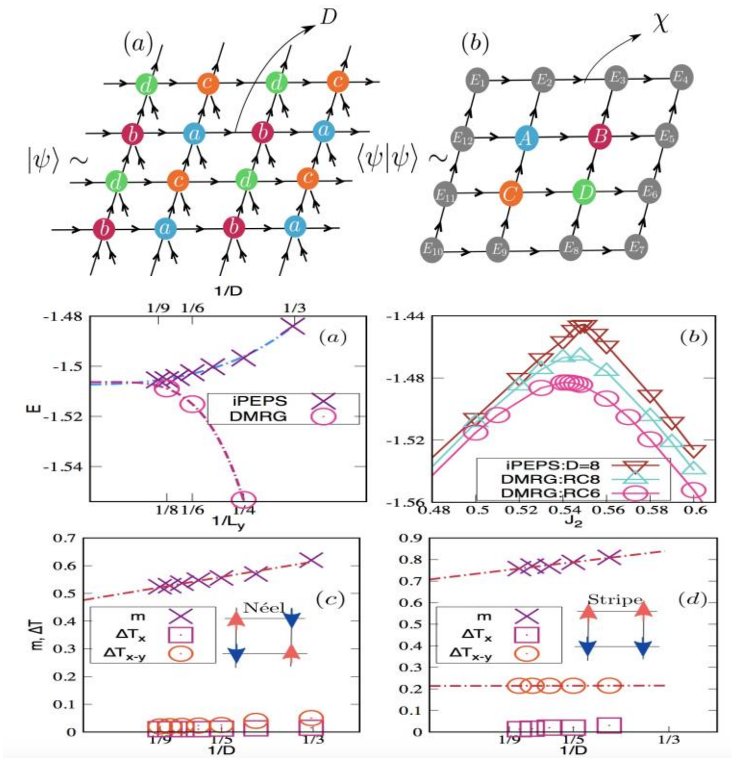

Caption: Top row shows the Tensor-network and its environment tensors. Middle row shows the accuracy in comparison to DMRG. The bottom raw illustrates identified order parameters for different quantum phases.

Reference

R. Haghshenas et al., Phys. Rev. B 97, 184436 (2018); R. Haghshenas et al., arXiv:1812.11436.

Scientific Achievement

By improving the algorithm, we demonstrate that tensor network can identify and characterize different frustrated systems including gapped chiral spin liquid.

Significance and Impact

Advancement in tensor network algorithm allows accurate simulations of strongly correlated quantum states of infinite systems.

Research Details

– We successfully apply U(1) symmetry, and corner transfer matrix method combined with one-layer contraction to spin systems, obtaining reliable quantum phase diagrams.

– We demonstrate that such tensor network can also faithfully represent time reversal symmetry breaking chiral spin liquid with the increase of the bond dimension.

U.S. DEPARTMENT OF ENERGY | Office of Science

Work was performed at CSUN under the support of the DOE Contract No. DE-AC02-76SF00515 through SLAC National Accelerator Laboratory.